Unexpected Electrophiles in the Atmosphere - Anhydride Nucleophile Reactions and Uptake to Biomass Burning Emissions†

Max Loebel Roson,[a] Maya Abou-Ghanem,[b] Erica Kim,[a] Shuang Wu,[a] and Dylan Long,[a] Sarah A. Styler,[c] and Ran Zhao*[a]

Biomass burning is a significant contributor to atmospheric pollution, its emissions have been found to have adverse impacts on climate and human health. Largely, these impacts are dictated by how the composition of the emissions changes once emitted into the atmosphere. Recently, anhydrides have been identified as a significant fraction of biomass burning emissions, however, little is known about their atmospheric evolution, or their interactions within the burn plume. Without this understanding, it is challenging to predict the impact of anhydrides on biomass burning emissions, and by extension, their influence on climate and health. In this study, we investigate anhydrides as potentially unrecognized electrophiles in the atmosphere. Firstly, by exploring their reactivity towards important biomass burning emitted nucleophiles, and secondly, by measuring their uptake on the emissions themselves. Our results show that phthalic and maleic anhydride can react with a wide range of nucleophiles, including hydroxy and amino-containing compounds, such as levoglucosan or aniline. Additionally, using a coated-wall flow tube setup, we demonstrate that anhydrides reactively uptake to biomass burning films and influence their composition. The anhydride nucleophile reaction was found to be irreversible, proceeding without sunlight or free radicals and indicating it may occur during the day or night time. Furthermore, the reaction products were found to be water-stable and contain functional groups which enhance their mass and likely contribute to the formation of secondary organic aerosol, with knock-on climate effects. Overall, our study sheds light on the fundamental chemistry of anhydrides and their potential impacts in the atmosphere.

1 Introduction

As a source of both environment- and health-affecting emissions, biomass burning has garnered considerable focus over the past few decades.[1–5] Much of this attention has been focused on identifying the effects and evolution of biomass burning emissions in the atmosphere.[3,6,7] Additional efforts have been directed towards deconvoluting the composition of the emissions themselves, as it is highly variable between burns and likely responsible for its harmful effects;[4,5] however, the fluctuating emission composition makes identification efforts considerably more difficult. While the commonly - and relatively high abundance - emitted compounds are well established (such as cellulose and hemicellulose decomposition products), the largest fraction represented by numerous low-intensity species, is not.[3,8–13] Convoluting things further, primary organic aerosol will physically and chemically evolve in the atmosphere. Through reactions occurring inside particles, as well as interactions with gas-phase molecules, its composition and effects are additionally modified.[14–19]

Recent studies have demonstrated that photochemical processing of biomass burn plumes in the atmosphere leads to the formation of anhydrides through aromatic oxidation and furan chemistry.[20–25] Specifically, maleic and phthalic anhydride represent two significant primary emissions from the combustion of biomass.[26] Without taking their eventual formation in the atmosphere into consideration, the emission factors of these two anhydrides can surpass those of other significant tracer species, such as vanillin or anisyl alcohol.[10,26]

Ordinarily, reactive anhydrides such as maleic or phthalic anhydride would be expected to swiftly decay once emitted into the atmosphere through hydration into their acid form.[22,27] In fact, both maleic and phthalic acid have been previously detected as a fraction of particulate matter.[28–31] However, anhydrides have been shown to remain inside burn plumes over several days.[25] While traveling inside a plume or bound to particulate matter, anhydrides can be shielded from environmental effects that would typically degrade them, such as moisture or sunlight.[32,33] Due to this increased atmospheric lifetime, anhydrides have been considered as potential tracers for aged biomass burning plumes,[25] which have historically been source apportioned by atmospheric modelers using species such as levoglucosan.[34–36]

In solvents, electrophilic anhydrides readily react with an assortment of nucleophiles. The mechanism for the acid catalyzed nucleophilic addition of water to an acid anhydride is depicted in Figure 1, ester and amide formation paths shortened.[37] The acid catalyzed path is favoured in the atmosphere, where the majority of available water is acidic in nature.[38] Similarly to Figure 1, heterocyclic anhydrides such as maleic and phthalic anhydride also hydrolyze under addition of water, forming instead dicarboxylic acids with higher molecular weight than their precursors. Corre-

[a] Department of Chemistry, University of Alberta, Edmonton, Alberta T6G 2G2, Canada; E-mail: rz@ualberta.ca
[b] NOAA Chemical Sciences Laboratory, Boulder, United States of America; E-mail: maya.abou-ghanem@noaa.gov
[c] Department of Chemistry & Chemical Biology, Hamilton, L8S 4M1, Canada; E-mail: stylers@mcmaster.ca

† Electronic Supplementary Information (ESI) available: Additional experimental details, including NMR plots, gas-phase anhydride determination, LC-MS chromatograms, burn and uptake parameters, standard and replicate analyses, and nucleophile product data.

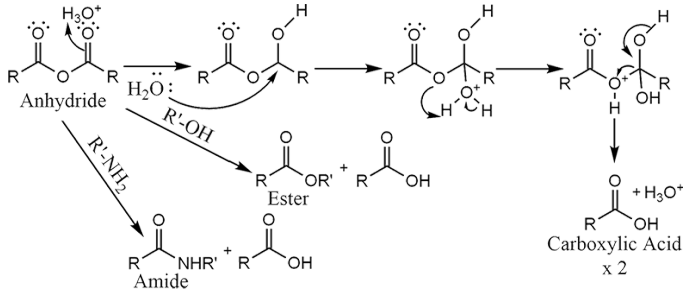

Fig. 1 Acid catalyzed acid anhydride nucleophilic addition reaction, alcohol and amine driven additions are simplified.

spondingly, they may also react with alcohol and amine containing nucleophiles to form products which contain both a carboxylic acid functional group in addition to an ester or amide group respectively.

With greater mass and inhibited volatility, these compounds are likely to contribute to secondary organic aerosol, enhancing the impact of biomass burning on air quality and climate.[8,39] However, since the composition of biomass burning particulate matter has not been fully established, the identity of these nucleophiles, the outcome of their reaction with anhydrides, and their ultimate environmental fate remains largely unknown and unpredictable. Nonetheless, to react with particle-bound nucleophilic species, anhydrides need to first be uptaken to the surface of biomass burning particulate matter. Heterogeneous uptake of gas-phase species by particulate matter is an important consideration in atmospheric research, as it has been shown to impact particle optical and cloud forming capabilities, as well as the distribution of gas-phase species in the atmosphere.[40] Carbonaceous particles such as those emitted from biomass burning have a significant surface area to size ratio,[41] which promotes uptake as both a physical (through absorption and adsorption, also known as bulk and surface accommodation respectively) and chemical process (through which the species react with the substrate itself, also known as reactive uptake).[40,42–45] However, to our best knowledge, the uptake of anhydrides to particulate matter, including that arising from biomass burning, has never been studied. Identifying and quantifying the propensity for uptake anhydrides possess is imperative towards understanding their reactions on the surface of biomass burning particulate matter. And ultimately, determining whether these processes are forming distinct product classes, in addition to the fate of compounds anhydrides readily react with.

Herein, we posit that anhydrides are unrecognized and environmentally relevant electrophiles in the atmosphere, and have conducted a series of laboratory experiments to assess this hypothesis. In particular, we aimed to examine whether anhydrides would react with nucleophiles emitted from biomass burning, and how variable conditions (such as available water) would affect this reaction. Also, we sought to determine if anhydrides would be capable of accessing nucleophiles present in biomass burning emissions in the first place - through uptake - and whether this process is reactive. We demonstrate that anhydrides emitted from biomass burning readily react with a variety of chemical species - including levoglucosan, a major biomass burning tracer - present in biomass burning emissions; and form low-volatility, water-stable products. These properties, coupled with their propensity to be strongly uptaken by biomass burning emissions, may make anhydrides significant model compounds to probe gas-phase interactions at the surface of biomass burning emissions in the future.

2 Materials and Methods

2.1 Choice of Anhydrides and Nucleophiles

Anhydrides are significant contributors of total emissions from biomass burning.[23] Maleic (99% purity, purchased from Sigma Aldrich) and phthalic anhydride (99+% A.C.S Reagent, Sigma Aldrich) were chosen as two of the major anhydrides observed in biomass burning emissions.[23,26] Maleic anhydride is the end product of furan chemistry,[23] while phthalic anhydride mostly forms through oxidation of naphthalene.[26] Phthalic anhydride is a precursor for phthalic acid,[23,26] which has been identified as a secondary organic aerosol constituent of aged biomass burning emissions,[46,47] and suggested as a proxy for the contribution of secondary organic aerosol to ambient samples.[48–50] The chosen nucleophilic species (referred to further as nucleophiles) represent only a few of the major emissions from biomass burning, and were selected due to their previous detection in Loebel Roson *et al.*.[13] Levoglucosan (99%, Sigma Aldrich), coniferyl aldehyde (98%, Sigma Aldrich), anisyl alcohol (98%, Sigma Aldrich), and vanillin (99%, ReagentPlus, Sigma Aldrich) are all common biomass burning tracers which represent a variety of functional groups and molecular properties.[10,28,34,35,51] Histidine (99%, ReagentPlus, Sigma Aldrich) is an essential amino acid present in animal dung, which is used as fuel for cooking and heating in numerous developing countries.[52] Additionally, to study the interactions between anhydrides and nucleophiles extrinsic to biomass burning emissions, a few species of anthropogenic origin were also studied. These species included aniline, chosen as the simplest aromatic amine (≥99.5%, A.C.S Reagent, Sigma Aldrich), and triethylene glycol, as a highly oxygenated volatile organic compound (99%, ReagentPlus, Sigma Aldrich).

2.2 Nucleophlic Addition in the Condensed Phase

To test the propensity of anhydrides to undergo nucleophlic addition reactions in the condensed phase, a series of fundamental analyses were performed in solvents. The atmospheric condensed phases can be highly variable in their water contents. Organic aerosol can have minimal liquid water content under dry conditions, while cloud and fog are made of aqueous droplets. With high water availability, it is possible for the anhydride hydrolysis to take precedence over other nucleophilic addition reactions. As such, solutions were prepared in water and acetonitrile (ACN), with differing fractions of each solvent ranging from 0 to 99 % (v/v) water. ACN was employed as an aprotic solvent that does not react with anhydrides. The stability of anhydrides in protic and aprotic solvents were examined using proton nuclear magnetic resonance (^{1}H NMR) spectroscopy. Each standard was dissolved to a concentration of 1 mM in both deuterated water (pro-

tic) and deuterated chloroform (aprotic), for a total of 8 samples per analysis. Each sample was spiked with a known concentration (0.5 mM) of dimethyl sulfoxide to act as an internal standard for chemical shift calibration and quantification, and analyzed after resting overnight. ^{1}H NMR chemical shift spectra are included in the Supplementary Information (S.I.1).

The nucleophiles and anhydrides were separately dissolved - in water and ACN respectively - to avoid premature formation of the acid. Following, maleic or phthalic anhydride dissolved in ACN were added to an aliquot of each nucleophile standard. In each solution, the final concentration of the nucleophile and the anhydride was 0.8 mM and 0.08 mM respectively. To evaluate the stability of the formed products, solutions were left to rest enclosed under room light and temperature for up to a week after mixing. Liquid Chromatography Mass Spectrometry (LC-MS) injections of each solution were performed after 24 hours and 1 week. Solutions were separated on a Luna Omega 3 μm Polar C18 100 Å column (150 $\times$ 2.1 mm) purchased from Phenomenex Inc. The mobile phase consisted of 50% water and 50% ACN, both buffered with 0.05% formic acid, and kept isocratic throughout the 8 min separation. Negative electrospray ionization mode (ESI-) was used for ionization. Ion detection was conducted on a linear ion trap mass spectrometer (model LTQ XL, Thermo Scientific). LC-MS data were analyzed on the Thermo Scientific FreeStyle software (v. 1.7.73.12)

2.3 Uptake Experiments

Uptake of reactive gaseous species can be monitored by a few methods as outlined in Kolb *et al.*.[40] In its simplest form, uptake is measured as the difference in initial versus final gas-phase mixing ratio of a compound of interest after passing through an absorptive or adsorptive device, typically a coated flow tube or Knudsen cell of known dimensions.[40] The uptake setup is depicted below in Figure 2. Two mass flow controllers (MFCs) are used to adjust the flow of dry zero air through the system. The first MFC adjusts the airflow through a glass cell containing 0.03-0.04 g of a solid anhydride. Gas-phase anhydride is continuously generated as the air flow causes steady vaporization of anhydride molecules. This MFC therefore modulates the quantity of gas-phase anhydride flowing through the glass tubes. The second MFC regulates the humidity of the total airflow by flowing zero air through a water bubbler. The ratio of humidified to dry air dictates the final relative humidity (RH) of the total airflow, which is monitored using an RH and temperature sensor before the Gas Chromatography Flame Ionisation Detection (GC-FID) inlet.

As can be seen in Figure 2, the anhydride initially flows through an uncoated glass tube into the GC-FID. A gas sampling valve inside the GC inlet port samples the anhydride continuously. Detection is achieved with the following parameters: Split injection 6:1, 100 °C injection temperature, 250 °C FID temperature, oven initial temperature set to 60 °C and held for 0.2 min, ramp rate set to 125 °C per min up to 150 °C and held for 0.2 min for a total run time of 1.250 min. A RTX-5 capillary column (7 m, 0.32 mm I.D., 0.25 μm film thickness, Thermo Scientific, CA) was used for separation. Including the time needed for the instrument to cool down between runs, an anhydride peak signal is obtained every 2.7 min.

Stabilization of the anhydride GC-FID signal typically occurs over the course of $\sim$2 hours and is measured using the height of the signal peak. The stabilized gas-phase concentration was estimated using the water bubbler under a differing experimental setup and is described in the Supplementary Information (S.I.2). Once stabilized, the flow is switched through the first three way valve to a tube coated with biomass burning emissions, the collection and coating of which are described in following sections. The uptake of anhydride is derived by measuring the decrease in the GC-FID signal relative to the initial signal over the course of 2 hours, when the signal approaches steady-state. After this point, the flow is once again switched to the uncoated tube for 2 more hours, totaling to a 6 hour experimental run time. RH and temperature are measured before and after each experiment by diverting the flow through a sensor, no significant changes in RH or temperature were observed within this time frame.

To date, gas-phase phthalic anhydride ambient air measurements have not been reported, while maleic anhydride concentrations are sparsely reported.[23,24,53] Lee *et al.* have performed ambient particle measurements showing variable concentrations of phthalic anhydride of $\sim$ 49.9$\pm$47.7 ng m^{-3}.[54] The lack of ambient data is in part due to the anhydride concentration being negligible after plume dissipation, combined with requiring high resolution instrumentation for their detection which is typically not employed for routine analyses. Instead, anhydrides are usually detected as part of the complex plumes emitted after burn events, when their concentrations spike. The predicted phthalic anhydride mixing ratio within our system is 4-10 ppb, which is closely associated with previous reports of $\sim$1-2 ppb for maleic anhydride in aged burn plumes.[23,24,53] However, the mixing ratio of maleic anhydride was estimated to be 2-7 ppm, lowering this concentration while maintaining reproducibility was challenging due to its high volatility. For this reason, only phthalic anhydride uptake coefficients are reported following. Nevertheless, maleic anhydride is expected to uptake more strongly than phthalic anhydride, and is still employed for alternative experiments in the previous and following sections.

By modifying the composition of the coated tube, the mass loading, RH effect, as well as coating with an uncoated tube (blank), an unreactive material (linoleic acid), or with an anhydride reactive one (dopant) were all studied.

2.4 Coating Material Collection and Solid Fuel Burning

Samples were collected as previously described in Loebel Roson *et al.*,[13] briefly, a tube furnace was used to reproducibly burn and collect wood (lodgepole pine) biomass burning emissions on pre-baked 0.22 μm pore size quartz fiber filters. After collection, whole filters were extracted in 10 or 20 mL of ACN using a magnetic stirrer for 40 minutes. To ensure homogeneity of the coating material, a composite sample, combining 4 filter extracts of separate burns, was employed for the coated tube uptake experiments. The exact burn parameters and filter loading information can be found in the Supplementary Information (Table S.I.2). In addi-

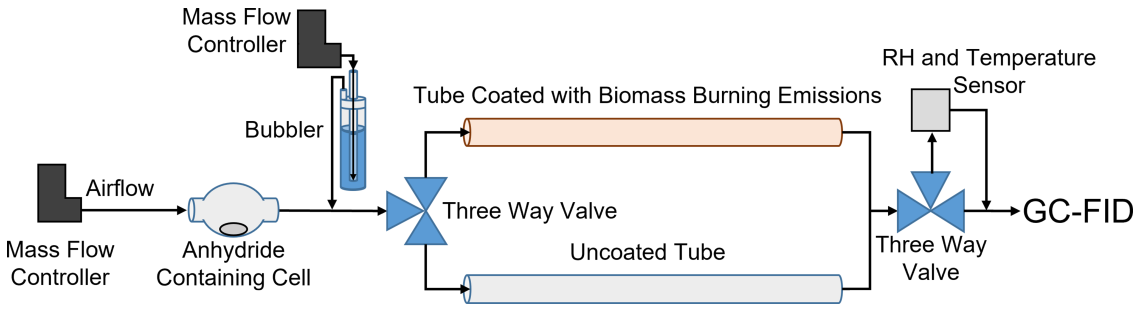

Fig. 2 Anhydride uptake experimental setup.

tion to the biomass burning materials, we have also used linoleic acid as a coating material in selected experiments. Linoleic acid serves as a surrogate for an unreactive coating towards which anhydrides should display only physical uptake, it has been employed in a number of previous studies.[55–59]

2.5 Tube Coating

Before uptake, glass tubes (200 mm long, 9.50 mm inner diameter) were coated with the filter extracts described above. To ensure uniform coating, the glass tubes were placed on a rotating hot dog roller (Nostalgia HDR8RR Retro Hot Dog Warmer 8) with the heating plate disabled. A pre-defined volume (0.6 to 7.2 mL) of extract was slowly pipetted into the rotating tube. This volume was used to calculate the mass loading of the coating. For select experiments, a dopant - usually a strong nucleophile (e.g., levoglucosan) - was also pipetted into the rotating tube. The dopant serves to modify the uptake properties of the coating and promote the formation of the anhydride nucleophile product. A constant flow of dry air was blown through the revolving tube to remove the ACN solvent. As the tubes rotate, the extracts are uniformly coated along their inner surface. After 30 minutes, at which point the liquid appears visually removed, the rotation function of the roller was disabled.

Our biomass burning materials represent primary organic components collected directly from the source, which contain a substantial quantity of semivolatile organic compounds. In the atmosphere, these semivolatile species are expected to undergo partitioning into the gas phase following plume dilution.[40] To ensure the removal of semivolatile organic compounds from the coating, the tubes were then rested with continued airflow for 24 hours before the uptake experiments were performed. Tube loading mass was back-calculated under the assumption that the entirety of the filter particulate matter was extracted into the liquid matrix and that the fraction of removed semivolatile organic compounds is the same between coatings.

2.6 LC-MS Analysis of the Coating Material

After performing the uptake experiments, each of the glass tubes were washed with 5 mL of ACN to remove the coated material. For select tubes, this material was recovered and diluted into LC-MS vials for analysis. Maleic and phthalic anhydride standards were used to confirm the presence of the anhydride, and detected as their corresponding acids using LC-MS. Separation, detection, and data analysis were performed as described in Section 2.2.

2.7 Uptake Calculations

Based on the uptake experiments, the uptake coefficients (γ) of the two anhydrides to biomass burning materials were calculated. The obtained γ is the net probability a molecule will be uptaken by a surface after colliding with it.[44,60,61] It is the most common parameter used for a wide range of reactive gaseous species.[40] In this work, the uptake was obtained using the peak signal of the anhydride of interest detected through GC-FID, under the assumption that the GC-FID signal is proportional to the gas-phase concentration of the anhydride. The effective uptake (γeff) values are normalized by the average gas kinetic flux and are determined as described by Knopf, Poeshl and Shiraiwa (KPS Method),[62] using Eqn (1):

$$\gamma_{eff,X} = \frac{D_{tube}}{\omega_x t} \ln\left(\frac{[X]_{g,0}}{[X]_g}\right) \quad (1)$$

Where D_{tube} is the diameter of the tube, t the residence time inside the flow tube, and $[X]_{g,0}$ and $[X]_g$ the initial and final gas phase concentration respectively, which we substitute here with the initial and final GC-FID signal. The molecular velocity (ω_x) can be calculated using Eqn (2):[63]

$$\omega_x = \sqrt{\frac{8RT}{\pi m}} \quad (2)$$

Where, R is the ideal gas constant (8.3145 J K^{-1} mol^{-1}), m the molar mass of particles (0.1481 kg/mol for phthalic anhydride), and T the temperature (296.15 K).

The KPS method corrects for the establishment of concentration gradients as a result of flow entrance effects into the coated tubes, which may cause overestimation of γ.[62,64]

To derive which parameters limit the uptake mechanism of a specific species it is useful to identify the gas flow regime occurring inside the flow tube, which is described by the Knudsen number (Kn_x).[44,62] Air flow through the uptake tube was found to be laminar using the Reynolds number (Re) and established after less than 1 cm of tube length.[65] Under laminar flow, the uptake mechanism is driven by molecular diffusion depending on the flow regime.[62] In turn, there are typically three possible flow regimes.[44] The flow of a given species from the gas phase

to the surface is limited either only by surface interactions (free-molecule regime, when $Kn_x >> 1$), by gas-phase diffusion (continuum regime, when $Kn_x << 1$) or by both gas-phase diffusion and uptake (transition regime, $\gamma \approx 1$ or if $Kn_x << 1$ and $Kn_x/\gamma \approx 1$).[44,62] Consequently, the flow of the anhydride in the experimental setup is usually limited by gas phase diffusion ($Kn_x << 1$). However, heavily loaded tubes can approach the transition regime and therefore be limited by both gas phase diffusion and uptake ($Kn_x << 1$ and $Kn_x/\gamma \sim 2$). Under either of these conditions, the effective uptake was corrected for diffusion effects (obtaining γ) by using the Kn_x and Sherwood (Shw) numbers as per KPS, as shown in Eqns (6-3).[62,66] Calculations for each of the parameters and their experimental values are included in the Supplementary Information (Table S.I.3).

$$\lambda x = \frac{3D_{g,X}}{\omega_x} \tag{3}$$

$D_{g,x}$ is obtained for each anhydride as described by Tang *et al.*.[63]

$$Kn_x = \frac{2\lambda x}{D_{tube}} \tag{4}$$

$$N_{Shw}^{eff} = 3.6568 + \frac{A}{z^* + B} \tag{5}$$

A and B are constants (0.0978 and 0.0154 respectively),[62] the dimensional axial distance (z^*) for the flow tube setup was calculated to be 0.651.

$$\gamma_x = \frac{\gamma_{\text{eff,X}}}{1 - \gamma_{\text{eff,X}} \frac{3}{2N_{Shw}^{eff} Kn_x}} \tag{6}$$

Both γeff and γ describe the net movement of anhydride from the gas phase to the coated tube surface. γ however, is normalized (corrected) by the actual surface collision flux rather than the average gas kinetic flux.[44] Herein, the KPS factor typically corrected the γeff values by ~5-12%, with the highest corrections being 20 and 21% for the two most heavily loaded tubes.

3 Results and discussion

3.1 Fundamental Investigation of Nucleophilic Addition

3.1.1 Anhydrides in Protic and Aprotic Solvents - NMR Characterization

To verify that anhydrides are both fully hydrolyzed in water and remain stable in aprotic environment, we characterized the formation of their acid counterparts in different solvents using ^{1}H NMR. Throughout the NMR experiments, a distinct acid peak was observed for all samples, except for the anhydride samples dissolved in deuterated chloroform, an aprotic solvent. Complete hydrolysis of the anhydride was confirmed by the lack of an anhydride peak in the deuterated water samples, as well as the acid peak intensity for all samples being analogous. Additional details for this experiment, including nuclear magnetic resonance peaks, are available in the Supplementary Information (S.I.1).

3.1.2 Reaction Confirmation using LC-MS

As electrophiles, anhydrides have a predisposition towards reacting with nucleophilic species. Significant tracers emitted from biomass burning - such as vanillin and levoglucosan - are nucleophiles and can be reactive towards anhydrides. As a basis for the uptake and degradation experiments, the formation of an anhydride and nucleophile product was first probed in an aprotic solvent. Table 1 lists the product peaks (anhydride + nucleophile) of species observed using LC-MS after mixing each anhydride with a variety of nucleophiles dissolved in ACN.

Both maleic and phthalic anhydride consistently form products with the majority of nucleophiles studied here. This reaction involves a hydrolysis-like ring opening of the anhydride and addition of the nucleophile to form a higher molecular mass product, which appears to be independent of the anhydride used. Likely due to its higher ionization efficiency, product peaks of maleic anhydride displayed ~10 times the peak area of phthalic. Maleic and phthalic anhydride were found to react with biomass burning atmospheric tracers such as levoglucosan, syringaldehyde, anisyl alcohol, and vanillin. The m/z of all the products were equivalent to the combined molecular mass of the anhydride and the corresponding nucleophile (see Supplementary Information (Figure S.I.9) for predicted structures). The list presented in Table 1 is nonexhaustive, and our results suggest that a wider spectrum of compounds in actual biomass burning plumes are likely reactive to anhydrides. Certain nucleophiles, such as aniline and levoglucosan, do not contain any acidic protons and are not detectable by ESI- themselves. The fact that the products are detectable suggests the presence of an acidic functional group (i.e., carboxyl group), which is in agreement with the general reaction scheme and supports our structural assignment. After observing these reactions in ACN, whether anhydrides can react with nucleophiles of biomass burning origin in water - a protic solvent - and whether the products of such a reaction are stable is explored further.

Table 1 Maleic (M) or phthalic (P) anhydride nucleophile reaction products detected using LC-MS. In each instance, the listed ionization method and product peak mass to charge (m/z) were those that yielded the highest intensity LC-MS signals.

Nucleophile	Anhydride	Product Peak (m/z)
Anisyl alcohol	Both	236 (M) and 286 (P)
Coniferyl aldehyde	M	276 (M)
Histidine	Both	253 (M) and 303 (P)
Levoglucosan	Both	260 (M) and 310 (P)
Vanillin	Both	250 (M) and 300 (P)
Aniline*	Both	190 (M) and 241 (P)
Triethylene glycol*	Both	248 (M) and 298 (P)

*Compounds not detected in biomass burning emissions in Loebel Roson *et al.* [13]

3.1.3 Reaction Competition and Product Stability in Water

Since anhydrides fully hydrolyze when dissolved in water, the potential for competition between hydrolysis and the anhydride nucleophile reaction was explored further. Depending on local atmospheric conditions, biomass burning emissions are subjected to a spectrum of relative humidities.[8,38,39,62] Water can impact reactions at the surface and bulk of the particle phase, and through hydrolysis - along with photolysis and oxidation - is one of the main mechanisms leading to the decomposition of certain chem-

ical species in the atmosphere.[67] To study whether the size of the water fraction hinders the formation of the anhydride nucleophile product and if that product is stable in water over time, the evolution of the product was tracked in increasing fractions of water in ACN, as described in Section 2.2. By comparing the relative area of the product peak over each injection, whether the product is forming or decaying is determined. Anisyl alcohol, levoglucosan and vanillin were selected as nucleophiles for this analysis, as they each represent significant biomass burning tracers.[10,28,35] Data for maleic anhydride and vanillin, as well as for phthalic anhydride and levoglucosan are presented in Figure 3. Data for other anhydride nucleophile products is available in the Supplementary Information (S.I.7). Anisyl alcohol followed a similar trend to levoglucosan curves in Figure 3, albeit with an even higher product signal intensity.

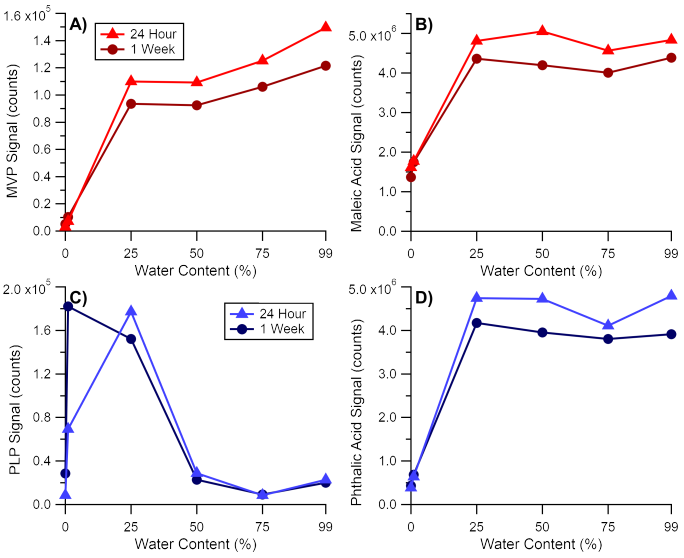

Fig. 3 LC-MS peak area signals obtained from increasing fractions of water in acetonitrile (ACN) after the 24 hour and 1 week-long analysis period for A) Maleic anhydride vanillin product (MVP), B) Maleic acid, C) Phthalic anhydride levoglucosan product (PLP), D) Phthalic acid.

As displayed in Figure 3, anhydride hydrolysis becomes dominant when the water content exceeds 25%. This is illustrated by the sharp rise in acid signals - i.e., maleic acid (Figure 3B) and phthalic acid (Figure 3D), which the previously reported NMR analysis also corroborates. On the other hand, the evolution of the nucleophile product follows a non-linear trend. This indicates that the presence of water is playing a more complex role in its formation. For both the maleic anhydride vanillin product (MVP) (Figure 3A) and phthalic anhydride levoglucosan product (PLP) (Figure 3C) systems, up to 25% water facilitated the formation of the products. As can be seen in Figure 1A, a proton must migrate from the nucleophile to the newly formed carboxylic group. Likely, water may act as a proton carrier during the nucleophilic addition, resulting in the enhanced product formation observed in Figures 3A and 3C. Specifically for 3C, 1% water is enough to initiate proton transfer and the formation of PLP - albeit at a much slower rate - leading to a maxima over 1 week. The acid catalyzed reaction path (Figure 1B) is also promoted with an increased water fraction, as more acidic protons become available.

Opposing trends were observed between the two experimental systems after increasing the water fraction beyond 25%. The PLP intensity diminishes at higher water contents, indicating that hydrolysis competes over the nucleophilic addition. Simultaneously, the MVP signal exhibits a continuous enhancement with water content. This trend is likely an interplay of multiple factors, including the reactivity of the anhydride, the nucleophilicity of vanillin, and their concentrations relative to each other in the solution. Nonetheless, we were unable to identify the exact reason for this observation within the MVP system.

These experiments also gauge the stability of the products in water. As shown in Figures 3A and 3C, the product signals exhibited minimal (<10%) reduction over a 1 week time frame. A decrease of the same magnitude was observed for the acids (Figures 3B and 3D), indicating the decline might be due to changes in instrumental sensitivity between analyses. In either case, the products remain stable in water once formed. This confirms that the anhydride nucleophilic addition reaction is irreversible. Overall, our observations indicate that water serves to facilitate the nucleophilic addition to anhydrides when it does not represent the majority of the medium. This corresponds to dry atmospheric conditions under which liquid water in aerosol is scarce and dependent on ambient relative humidity and the hygroscopicity of the aerosol itself.[68] When water becomes abundant, hydrolysis eventually overtakes the nucleophilic addition. However, our results also demonstrate that certain nucleophiles can still react under such conditions, and form products that are stable and do not decompose in water. For anhydrides and nucleophiles to react, they must first come into contact with each other. A controlled liquid environment facilitates observing the reaction, and is useful as a proof of principle. Inside a burn plume however, gas-phase anhydrides must first interact with the surface of biomass burning emissions before reacting with particle-bound nucleophilic species. In the following section, we explore whether anhydrides show a susceptibility for surface and bulk uptake on biomass burning films.

3.2 Uptake of Anhydrides to Biomass Burning Material

3.2.1 Uptake of Phthalic Anhydride

Figure 4 depicts a typical phthalic anhydride uptake experiment. The top panel displays a single phthalic anhydride GC-FID chromatogram, while each point on the bottom chromatogram represents the height of the anhydride peak measured in real time by the GC-FID, as exemplified by the green marker in each panel. Each uptake experiment was divided into three regions as described in the experimental section, represented by the shaded areas in the figure. Initially, the anhydride equilibrates throughout the uncoated tube over the course of $\sim$ 100 minutes (gray shade). After equilibration, a three-way valve is switched, and the anhydride is flown through the coated tube (red shade). The GC-FID signal begins decreasing over the course of a single injection (2.7 min) and usually reaches a minimum after 6-8 injections (16.2-21.6 min). From here, the signal begins slowly increasing as the surface of the tube is saturated with anhydride. Once the anhy-

dride flow is switched back to the uncoated tube (gray shade), it re-equilibrates over a further 100 min.

γ can be calculated for different positions of the uptake curve. As the largest uptake occurs during the initial switch to the coated tube, γ determined by the difference between the initial and final GC-FID signals yields initial uptake. γ calculated over the entire experiment, i.e., over the entirety of the red shaded area in Figure 4, represents the averaged uptake. Unless specified otherwise, all γ values reported denote the average uptake. The molecular mass of an uptaken trace gas strongly influences the speed and degree of uptake.[63] As relatively large molecules - over the more commonly studied gas phase oxidants OH, O_3 and NO_3[62,64] - maleic and phthalic anhydride are expected to follow a slower uptake profile with reduced average uptake.

It is worth noting that γ is theoretically unaffected by the gas-phase concentration of the uptaken trace-gas as it simply measures the difference between the initial and final concentrations of a gas after passing over a coated material. However, should the gas-phase concentration of the trace-gas be too high, or conversely, insufficient coating material (reactive sites) be available for uptake, γ may be over or underestimated. While the shape of the uptake curves is usually consistent, γ coefficients available in literature have a wide range of values due to the variable experimental conditions and correction method.[62,64,69–72] For example, in liquid coated reactive uptake setups, the concentration of the liquid will directly affect its total capacity for uptake when diffusion into the bulk is unlimited.[69] This phenomenon occurs when the number of reactive sites in the bulk are the limiting factor for uptake, and is observed here as the loading mass of the coated tubes is changed (see Section 3.3.1 - Mass Dependence). The shape of the phthalic uptake curve in Figure 4 is consistent with uptake experiments reported on in previous ozone studies and is - as expected - characteristic of sustained uptake.[62,64,72–74]

Table 2 lists the γ obtained as a function of the loading mass of the coatings. Also included are experiments with coated linoleic acid and variable RH, covered in sections 3.3.2 and 3.3.3, respectively. As can be seen in Table 2, uptake is driven by the quantity of coating applied to the tube, which directly correlates to the mass concentration of particles emitted from the burn. Therefore, it is reasonable to expect burns which emit a larger number of particles - such as large scale wildfires - to promote the uptake of anhydrides. The limited range of uptake values can be explained by the morphology of the uptake setup and the low diffusivity of phthalic anhydride. The comparatively low airflow and long tube length promote slow uptake and deposition of the anhydride on the sides of the glass tubes whether a coating is present or not.[64] This causes uncoated tubes to have $\sim$6 times less uptake than the most heavily loaded ones.

Table 2 Range of γ values obtained for phthalic anhydride during uptake as loading mass is decreased under variable relative humidity (RH).

Loading Mass (g)	Replicates	RH (%)	Uptake (γ) ($\times 10^{-6}$)
0.0127	2	0	10.87 - 11.44
0.042	3	0	5.77 - 6.98
0.032	3	0	5.44 - 6.55
0.032	2	24	5.50 - 5.66
0.032	3	47	5.24 - 6.49
0.021	2	0	4.05 - 4.51
0.011	2	0	2.63 - 2.69
0	3	0	1.07 - 2.43
0.0168*	1	0	1.78
0.0017*	1	0	1.85

*Tubes coated with linoleic acid

3.3 Evidence of Reactive Uptake

Differentiating between reactive and non-reactive uptake is challenging, as experimentally both types lower the relative concentration of gas-phase species being uptaken, yielding γeff coefficients. This is in part due to physical accommodation process being a pre-requisite for reactive uptake to occur. Nevertheless, physical and reactive uptake each modify the chemical composition of the uptake substrate in distinct ways. Reactive uptake can be reversible or irreversible, and has been shown to alter the properties of both the gas-phase species being uptaken as well as the uptake substrate itself.[40,75] For example, particulate matter emitted from biomass burning can act as a surface for the condensation of semivolatile species in the atmosphere.[75] As such, identifying whether anhydride reactive uptake is occurring and whether the products of such a reaction are stable is of high importance towards predicting their impacts.

We posit that significant reactive uptake is occurring on the biomass burning coating for the following reasons, each of which is expanded upon in their respective sections below.

1) A tube coated with the same loading mass of linoleic acid, towards which anhydrides are nonreactive, did not show significant uptake and no dependence on mass loading.

2) Products of the reaction of anhydrides and common biomass burning species (such as levoglucosan) were identified in tube coating extracts after uptake, and were shown to increase in concentration when the tubes were doped with the nucleophilic precursors.

3) A more reactive coating, from which semivolatile species were not removed before uptake, showed significantly higher γ.

3.3.1 Mass Dependence

Uptake is partially driven by the quantity of material loaded on the glass tubes, as can be seen in Figure 5 and Table 2. Loading mass represents the mass of particles originally collected on the quartz filters before extraction, except for the linoleic acid data-points, where it represents the mass of linoleic acid used for coating.

In either case, γ increases relatively linearly as the tubes are loaded with more material. A coating that covers the entirety of the glass tube - the surface area of which can not increase further - can only expand in depth as it is further loaded. Since γ increases with tube loading, uptake must be spurred by the transfer of the anhydride to the bulk of the coating. This is additional evidence of the reactive uptake process outlined in the previous sections. The divergence from linearity can be explained by the increasing resistance the coating thickness imposes on the uptake process and the depletion of readily available reactive sites. As

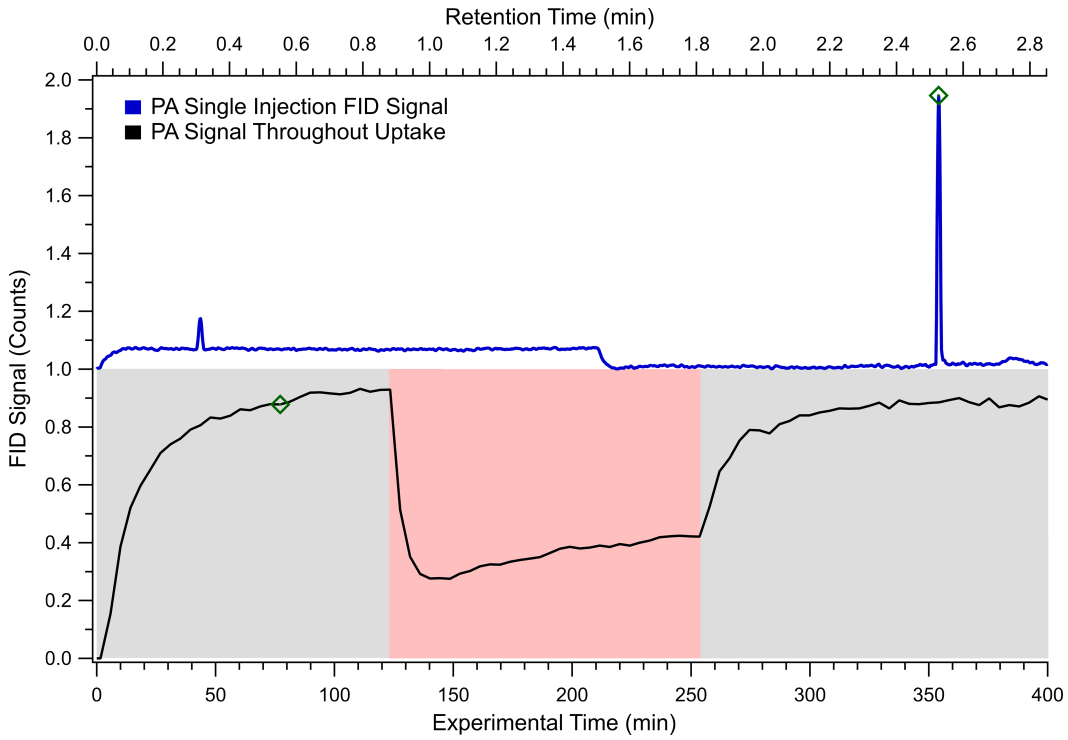

Fig. 4 Phthalic anhydride (PA) uptake experiment. The top blue curve represents a typical GC-FID PA peak vertically offset by 1 count, taken at 2.7 min intervals throughout the experiment and from which the bottom uptake graph is constructed. The bottom gray and red shaded areas represent the anhydride flowing through the uncoated and coated tubes respectively, γ is calculated over the length of the red area. The green marker on the bottom graph indicates the time at which the top peak is taken.

sites nearer to the surface are consumed first, the anhydride must travel deeper into the coating, creating a concentration gradient.

3.3.2 Linoleic Acid

To investigate whether the uptake process was purely physical or reactive, γ was also measured using tubes coated with linoleic acid, represented by the brown markers in Figure 5. Emitted from cooking processes, long chain unsaturated fatty acids such as oleic and linoleic acid have been previously used for model heterogeneous oxidation studies within an atmospheric context.[55–59]

Under a purely physical - adsorptive or absorptive - process, we can assume for comparison with the reactive biomass burning coating, that linoleic acid will either physically align itself along the surface of the tube in a single layer formation. That is to say, as a coating with no depth, in which case only adsorption would be possible. Or more realistically, that the linoleic acid coating does have depth, in which case both adsorption and absorption - also known as surface and bulk accommodation - are possible.[40,44,45] In either case, were the uptake on biomass burning emission coated tubes purely a physical process, then γ for linoleic acid should - with similar coating distribution - have a comparable uptake trend to it. However, as can be seen in Figure 5 no significant anhydride uptake to linoleic acid was observed over the loading mass range used for the biomass burning emissions. Therefore, we posit that the uptake is not only dependent on the physical properties of the biomass layer, but rather a chemically reactive process between the anhydride and the coating. This is further confirmed by both the effect removal of the volatile organic species had on γ (green dot), and the shape of the uptake curve in Figure 4.

3.3.3 Removal of Semivolatile Species

The presence of nucleophiles in biomass burning material is suspected to enhance the reactive uptake of anhydrides. Presumably, species which contain phenolic functional groups can serve as nucleophiles in the biomass burning substrate, and therefore heighten uptake. Due to their volatility, low-medium molecular weight phenolic species typically partition into the gas phase following plume dilution.[40] As a result of the sampling setup, the tube furnace may condense semivolatile species on the surface of the filter which would typically remain in the gas phase. Semivolatile removal time after coating was found to have a distinct impact on γ. The initial versus final GC-FID signal for phthalic anhydride flowing through a coated tube was found to experience a threefold reduction in γ after 24 hours of semivolatile removal, as displayed by the green dot in Figure 5. A similar trend was observed for maleic anhydride. The difference in uptake can be explained by the stripping of more semivolatile organic compounds from the coating over time. These species would usually provide additional sites for anhydride compounds to react with, but are instead removed under continued air flow, and therefore lower the overall reactive potential of the coating. Additionally, removal of the semivolatiles is likely to lower the overall volatility of the coating, increasing its viscosity, and inhibiting uptake.

Unsurprisingly, more freshly emitted biomass burning particulate matter is more reactive towards electrophiles such as anhy-

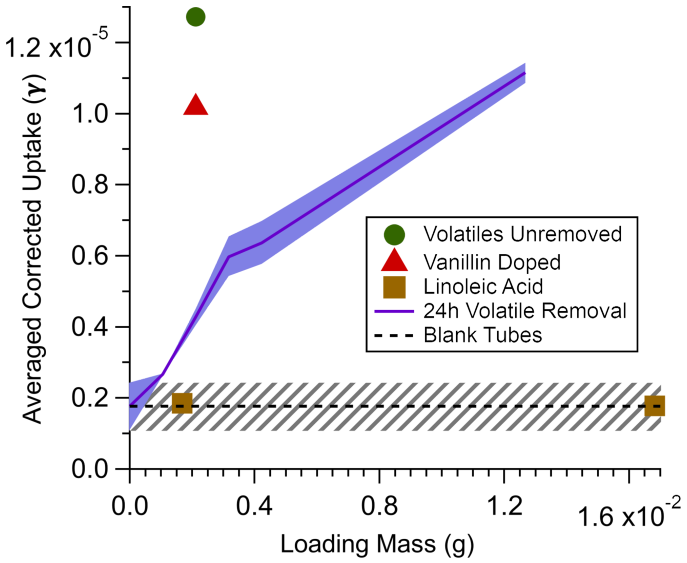

Fig. 5 Range of γ values obtained for phthalic anhydride on tubes coated with biomass burning material as a function of loading mass of the coating. Each data point represents the averaged γ values obtained over 2 hours of uptake at a relative humidity of 0. The shaded blue area depicts the range of γ values observed from tubes which underwent 24 hours of semivolatile removal. The green dot portrays the γ obtained from a tube which did not go through the semivolatile removal procedure. The red triangle represents the γ from a tube in which 0.0167 g of vanillin were dissolved during the coating process, in addition to the biomass burning material. The brown squares illustrate the γ obtained from tubes coated with linoleic acid, an unreactive material. The dashed line indicates the average γ obtained for uncoated (blank) tubes.

drides. Within the atmospheric context, freshly emitted biomass burning plumes which still contain semivolatile organic compounds will be more susceptible to reactive uptake, and therefore modification by anhydrides. Note that we cannot track the mass of semivolatiles lost during the 24 hour removal process, and thus assume that it is a minor fraction of the total biomass burning coating material. If the semivolatiles comprised a substantial fraction of the total mass, the data point (green circle) shown in Figure 5 would be underestimating the loading mass.

Interestingly, a few of these semivolatile species appear as unique GC-FID peaks when tubes which have not gone through the removal process are used for uptake. Figure 6 displays the phthalic anhydride GC-FID peaks obtained for a tube which has undergone the 24 hour removal process, and one which has not. Unsurprisingly, the unremoved coated tube continuously off-gasses volatile species from its surface throughout the uptake experiments. At the same time, the 24 hour removed tube displays only a single sharp peak, corresponding to phthalic anhydride. The peaks in Figure 6 represent only the species which are capable of eluting through the GC column in less than 2.8 minutes. Likely, there are numerous other peaks which could be observed beyond this retention time in the unremoved tubes.

3.3.4 Presence of Uptake Products - Tube Doping Experiments

To confirm the anhydrides react with the biomass coating, the tube coating was extracted from the surface after performing the

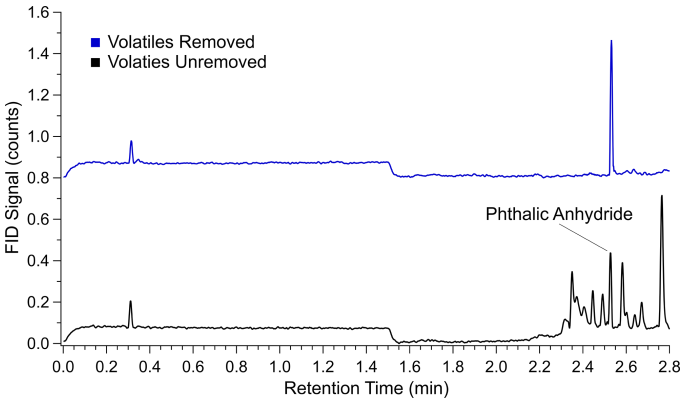

Fig. 6 GC-FID phthalic anhydride chromatogram of a tube rested under continued airflow for 24 hours versus a tube from which semivolatile species were not removed. The top peak signal is offset by 0.8 counts.

uptake experiments and analyzed using LC-MS. By spiking (doping) the tubes with commercially available nucleophilic precursors during the coating process, we further confirm the identity of the detections using LC-MS. Characterization is necessary as the biomass emission extracts are highly concentrated in a variety of chemically diverse compounds.[13,19] Despite separation through LC-MS, this environment makes it challenging to confirm the identity of a given product (using only the mass to charge ratio), without chemical standards. However, many of the species emitted from biomass burning either do not have commercially available standards or have not yet been identified. By doping, the surface concentration of the nucleophile is significantly higher, which promotes its reaction with the anhydride. Consequently, this results in the signal intensity of the obtained LC-MS reaction product peak - between the anhydride and the nucleophile - to also increase, confirming its identity within the complex extracts. This is further supported by doped tubes through which no anhydride is flown (containing the nucleophile but no uptaken anhydride), lacking the product peak.

Figure 7 displays the mass spectra gathered from two tubes coated with biomass burning emissions and doped with levoglucosan. One of the coated tubes underwent maleic anhydride uptake while the other did not. The TICs were gathered over a 2 min time range, and include the elution time of maleic anhydride, levoglucosan, and the maleic anhydride levoglucosan product (MLP). As can be seen in Figure 7, only the tube exposed to maleic anhydride displays peaks at mass to charges (m/z) of 115 (maleic anhydride detected as maleic acid), 259 (MLP), and 519 (MLP dimer). Notably, extractions were completed in an aprotic solvent (ACN), while the uptake was performed using air of 0% RH. As per the experiments in Section 3.1.3, formation of MLP is expected to increase further with moderate water availability.

A similar trend to that of the initial reactivity experiments was observed in this section, i.e. maleic and phthalic anhydride react with nucleophiles present in biomass burning emissions. Both biomass burning matrix intrinsic nucleophilic compounds with high emission factors (levoglucosan and vanillin) and matrix extrinsic anthropogenic nucleophilic compounds (aniline) were used as dopants. In either case, products corresponding to a mass

to charge ratio of the anhydride plus nucleophile were detected. In each instance, the product mass to charge ratio obtained after doping matched the one observed during the reactivity experiments. The signal intensity of the maleic anhydride products was significantly higher than the phthalic ones in all cases, likely due to its higher gas phase concentration during uptake. Formation of the products as anhydride is surface - and likely also bulk - accommodated on the tube coating, is further evidence of a reactive uptake process.

3.4 Additional Factors Affecting the Uptake - Relative Humidity

Relative humidity is an important consideration for atmospheric studies, as it affects the environmental fate, physical properties, and uptake potential of many chemical species. Organic aerosol particles in the atmosphere will change phase state between liquid and solid depending on local RH and temperature.[39] With regards to uptake, RH can decrease the viscosity of the uptake substrate, facilitating the movement of species into the bulk, which usually enhances the uptake.[75,76] More unusually, RH has also been found to hinder uptake in some systems. For example, Goldberger *et al.* have previously reported that γ of N_2O_5 to biomass burning aerosol emitted from longleaf pine needles is inhibited at higher RH, albeit only slightly.[77]

Here, uptake is expected to increase with RH, as lower viscosity improves anhydride transfer into the biomass burning coating. Further, as described in Section 3.1.3, water can either facilitate the nucleophilic addition, or react with the anhydrides through hydrolysis directly. Surprisingly, using air of either 0, 24, or 47% RH at room temperature was found to have no significant impact on γ, as can be seen in Table 2. Although a different system, a non-impact of RH has been previously reported for other gas-phase species. For example, under dark conditions, RH has no meaningful impact on steady-state uptake of ozone to a benzophenone film.[45,72] As covered in the experimental methods, the particles that make up the biomass burning coating are collected a few cm downstream of the tube furnace and represent primary emissions. A large fraction of freshly emitted biomass burning aerosol is made up of almost hydrophobic particles, which typically lose their hydrophobicity as they are aged and transported in the atmosphere.[64,78] During the tube coating process, dry air is used to remove semivolatiles and avoid hydrolysis-driven aging. It is likely that the hydrophobicity of the coating prevents the humidity in the air from lowering its viscosity over the $\sim$6 h time frame of the experiments, which nullifies the effect of RH on the uptake.

Presumably, biomass burning coated tubes exposed to humid air over an increased time period will experience an enhancement in anhydride uptake due to lowered substrate viscosity. However, this substrate would simulate particles which have undergone atmospheric aging. After exposure to humid air, these particles would have a chemical composition dissimilar from the fresher emissions which are the focus of the present study.

4 Conclusions

Using maleic and phthalic anhydride - compounds present in biomass burning plumes - this study provides novel insights into anhydride chemistry and its implications towards the atmosphere. Our results show that anhydrides can react with a wide spectrum of hydroxy and amino containing nucleophiles, corroborating established literature.[37,79] For the first time however, we demonstrate the reactivity of anhydrides towards atmospherically relevant nucleophiles, and that therefore, anhydrides may be a hitherto unrecognized class of electrophiles with atmospheric relevance.

Given the abundance of water in the atmospheric environment, it likely represents anhydrides' most dominant reaction partner, leading to the formation of their corresponding acids. However, our results show that reactions with other nucleophiles are possible even in the presence of water. In particular, lower water contents ($\sim$25 %) facilitated the nucleophilic reaction.

The chemistry of the anhydride can affect their own atmospheric fate as well as the composition of aerosol they come into contact with. We show, using a coated wall flow tube setup, that anhydrides reactively uptake to biomass burning films and influence its composition.

In addition, we show that the reaction is irreversible, and that therefore, reactive uptake to aerosol can serve as a sink for gas-phase anhydrides. The extent of this sink is dependent on the availability of nucleophilic species in the particle phase, as the uptake coefficient (γ) increased with tube loading mass. This effect is exacerbated by the ability of anhydrides to move from the surface into the bulk of the particle phase, where they may interact with additional fresher nucleophiles. Anhydrides have previously been considered as potential tracers for biomass burning.[23,25] However, their uptake properties combined with the non-discriminatory reactivity likely makes them a poor choice of tracer.

In addition to the uptake studies, products arising from the reaction between anhydrides and nucleophiles were monitored using LC-MS. Consistently, product peaks corresponding to ester and amide species which contain carboxylic groups were detected. Formation of such products has a few important atmospheric implications. Firstly, their enhanced molecular weight coupled to the added functional groups make them less volatile than their anhydride and nucleophile precursors. Based on our observations of their stability over a week-long time frame, these products are likely to persist in the particle phase and contribute to secondary organic aerosol, with knock-on climate and health effects. Secondly, this reaction does not require solar radiation or the presence of free radicals, which indicates that the reaction could proceed during day and night time. Thirdly, by reacting with compounds present in biomass burning aerosol, anhydrides may mask the "real" emission factor of nucleophiles. A symptom which may worsen as more anhydrides form through plume aging over time. This is potentially concerning for nucleophiles used as tracers, the concentration of which are used for source apportionment.[34–36] This effect would be more significant for anhydrides with emission factors higher than the nucleophile they

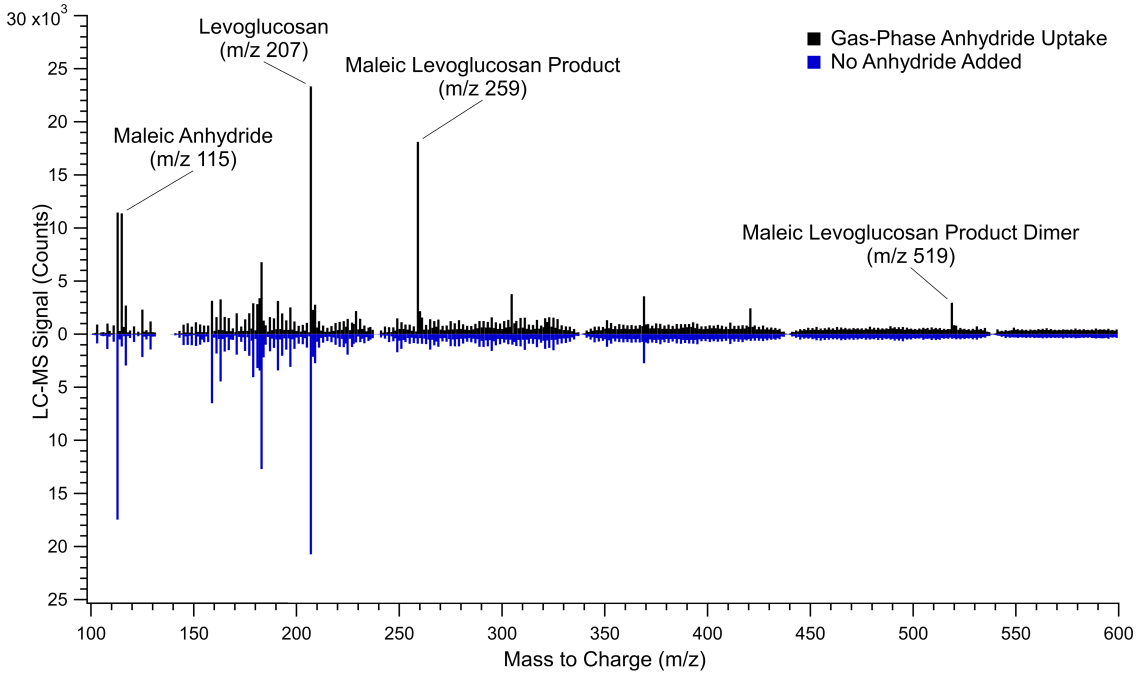

Fig. 7 Maleic anhydride levoglucosan product negative electrospray ionization (ESI-) total ion chromatogram (TIC) mass spectra. The top spectrum is gathered from a levoglucosan doped tube through which gas-phase anhydride was flown. The mirrored blue bottom spectrum tube was prepared under the same conditions, without the anhydride uptake step.

react with. For example, while emissions factors of phthalic anhydride and vanillin are comparable, [10,26] levoglucosan molecules greatly outnumber anhydrides inside a fresh burn plume, [10] likely rendering the masking of levoglucosan minimal. Such variability makes obtaining an accurate representation of both the reactions happening inside a plume, and their impacts, challenging.

As climate change proceeds, wildfire incidence and severity is expected to intensify. [80] Understanding chemical reactions leading to the continuous transformation of biomass burning emissions represents an area of significant interest and uncertainty. In this work, we investigated the fundamental chemistry and behavior of anhydrides, showing that they can potentially contribute to the chemical evolution of this type of emission. Future studies should focus on elucidating the complexity of the heterogeneous phase further, both as a physical and chemical process.

Author Contributions

Max Loebel Roson: Conceptualization, Methodology, Investigation, Visualization, Writing - Original Draft, **Maya Abou-Ghanem**: Resources, Validation, **Erica Kim**: Formal Analysis, **Shuang Wu**: Resources, **Dylan Long**: Resources, **Sarah A. Styler**: Supervision, **Ran Zhao**: Supervision, Writing - Review & Editing, Funding acquisition.

Conflicts of interest

There are no conflicts to declare.

Acknowledgements

The authors thank the University of Alberta Department of Chemistry Glass Shop for manufacturing the quartz and glass tubes. The authors also thank NSERC and the University of Alberta for financial support. This research was performed while co-author Maya Abou-Ghanem held an NRC Research Associateship award at NOAA Chemical Sciences Laboratory. This research project was partially supported by the Government of Canada's Climate Action and Awareness Fund, Canada Foundation of Innovation (Project Number 38334), and NSERC Discovery Grant (RGPIN2018-03814).

Notes and references

1 M. O. Andreae, *Atmospheric Chemistry and Physics*, 2019, **19**, 8523–8546.

2 J. Chen, C. Li, Z. Ristovski, A. Milic, Y. Gu, M. S. Islam, S. Wang, J. Hao, H. Zhang, C. He, H. Guo, H. Fu, B. Miljevic, L. Morawska, P. Thai, Y. F. LAM, G. Pereira, A. Ding, X. Huang and U. C. Dumka, *Science of The Total Environment*, 2017, **579**, 1000–1034.

3 S. K. Akagi, R. J. Yokelson, C. Wiedinmyer, M. J. Alvarado, J. S. Reid, T. Karl, J. D. Crounse and P. O. Wennberg, *Atmospheric Chemistry and Physics*, 2011, **11**, 4039–4072.

4 S. S. Lim, T. Vos, A. D. Flaxman, G. Danaei, K. Shibuya, H. Adair-Rohani, M. A. AlMazroa, M. Amann, H. R. Anderson, K. G. Andrews, M. Aryee, C. Atkinson, L. J. Bacchus, A. N. Bahalim, K. Balakrishnan, J. Balmes, S. Barker-Collo, A. Baxter, M. L. Bell, J. D. Blore, F. Blyth, C. Bonner, G. Borges, R. Bourne, M. Boussinesq, M. Brauer, P. Brooks, N. G. Bruce, B. Brunekreef, C. Bryan-Hancock, C. Bucello, R. Buchbinder, F. Bull, R. T. Burnett, T. E. Byers, B. Calabria, J. Carapetis, E. Carnahan, Z. Chafe, F. Charlson, H. Chen, J. S. Chen, A. T.-A. Cheng, J. C. Child, A. Cohen, K. E. Colson, B. C. Cowie, S. Darby, S. Darling, A. Davis, L. Degenhardt, F. Den-

tener, D. C. Des Jarlais, K. Devries, M. Dherani, E. L. Ding, E. R. Dorsey, T. Driscoll, K. Edmond, S. E. Ali, R. E. Engell, P. J. Erwin, S. Fahimi, G. Falder, F. Farzadfar, A. Ferrari, M. M. Finucane, S. Flaxman, F. G. R. Fowkes, G. Freedman, M. K. Freeman, E. Gakidou, S. Ghosh, E. Giovannucci, G. Gmel, K. Graham, R. Grainger, B. Grant, D. Gunnell, H. R. Gutierrez, W. Hall, H. W. Hoek, A. Hogan, H. D. Hosgood, D. Hoy, H. Hu, B. J. Hubbell, S. J. Hutchings, S. E. Ibeanusi, G. L. Jacklyn, R. Jasrasaria, J. B. Jonas, H. Kan, J. A. Kanis, N. Kassebaum, N. Kawakami, Y.-H. Khang, S. Khatibzadeh, J.-P. Khoo, C. Kok, F. Laden, R. Lalloo, Q. Lan, T. Lathlean, J. L. Leasher, J. Leigh, Y. Li, J. K. Lin, S. E. Lipshultz, S. London, R. Lozano, Y. Lu, J. Mak, R. Malekzadeh, L. Mallinger, W. Marcenes, L. March, R. Marks, R. Martin, P. McGale, J. McGrath, S. Mehta, Z. A. Memish, G. A. Mensah, T. R. Merriman, R. Micha, C. Michaud, V. Mishra, K. M. Hanafiah, A. A. Mokdad, L. Morawska, D. Mozaffarian, T. Murphy, M. Naghavi, B. Neal, P. K. Nelson, J. M. Nolla, R. Norman, C. Olives, S. B. Omer, J. Orchard, R. Osborne, B. Ostro, A. Page, K. D. Pandey, C. D. Parry, E. Passmore, J. Patra, N. Pearce, P. M. Pelizzari, M. Petzold, M. R. Phillips, D. Pope, C. A. Pope, J. Powles, M. Rao, H. Razavi, E. A. Rehfuess, J. T. Rehm, B. Ritz, F. P. Rivara, T. Roberts, C. Robinson, J. A. Rodriguez-Portales, I. Romieu, R. Room, L. C. Rosenfeld, A. Roy, L. Rushton, J. A. Salomon, U. Sampson, L. Sanchez-Riera, E. Sanman, A. Sapkota, S. Seedat, P. Shi, K. Shield, R. Shivakoti, G. M. Singh, D. A. Sleet, E. Smith, K. R. Smith, N. J. Stapelberg, K. Steenland, H. Stöckl, L. J. Stovner, K. Straif, L. Straney, G. D. Thurston, J. H. Tran, R. Van Dingenen, A. van Donkelaar, J. L. Veerman, L. Vijayakumar, R. Weintraub, M. M. Weissman, R. A. White, H. Whiteford, S. T. Wiersma, J. D. Wilkinson, H. C. Williams, W. Williams, N. Wilson, A. D. Woolf, P. Yip, J. M. Zielinski, A. D. Lopez, C. J. Murray and M. Ezzati, *The Lancet*, 2012, **380**, 2224–2260.

5 C. J. Murray, A. Y. Aravkin, P. Zheng, C. Abbafati, K. M. Abbas, M. Abbasi-Kangevari, F. Abd-Allah, A. Abdelalim, M. Abdollahi, I. Abdollahpour *et al.*, *The lancet*, 2020, **396**, 1223–1249.

6 J. S. Reid, R. Koppmann, T. F. Eck and D. P. Eleuterio, *Atmospheric Chemistry and Physics*, 2005, **5**, 799–825.

7 V. Vakkari, V.-M. Kerminen, J. P. Beukes, P. Tiitta, P. G. van Zyl, M. Josipovic, A. D. Venter, K. Jaars, D. R. Worsnop, M. Kulmala and L. Laakso, *Geophysical Research Letters*, 2014, **41**, 2644–2651.

8 A. Laskin, J. Laskin and S. A. Nizkorodov, *Chemical Reviews*, 2015, **115**, 4335–4382.

9 C. E. Stockwell, T. J. Christian, J. D. Goetz, T. Jayarathne, P. V. Bhave, P. S. Praveen, S. Adhikari, R. Maharjan, P. F. DeCarlo, E. A. Stone, E. Saikawa, D. R. Blake, I. J. Simpson, R. J. Yokelson and A. K. Panday, *Atmospheric Chemistry and Physics*, 2016, **16**, 11043–11081.

10 Y. Iinuma, E. Brüggemann, T. Gnauk, K. Müller, M. O. Andreae, G. Helas, R. Parmar and H. Herrmann, *Journal of Geophysical Research: Atmospheres*, 2007, **112**,.

11 P. Lin, N. Bluvshtein, Y. Rudich, S. A. Nizkorodov, J. Laskin and A. Laskin, *Environmental Science & Technology*, 2017, **51**, 11561–11570.

12 M. Claeys, R. Vermeylen, F. Yasmeen, Y. Gómez-González, X. Chi, W. Maenhaut, T. Mészáros and I. Salma, *Environmental Chemistry*, 2012, **9**, 273–284.

13 M. Loebel Roson, R. Duruisseau-Kuntz, M. Wang, K. Klimchuk, R. J. Abel, J. J. Harynuk and R. Zhao, *ACS Earth and Space Chemistry*, 2021, **5**, 2925–2937.

14 S. N. Pandis, R. A. Harley, G. R. Cass and J. H. Seinfeld, *Atmospheric Environment. Part A. General Topics*, 1992, **26**, 2269–2282.

15 J. H. Kroll and J. H. Seinfeld, *Atmospheric Environment*, 2008, **42**, 3593–3624.

16 M. Claeys, B. Graham, G. Vas, W. Wang, R. Vermeylen, V. Pashynska, J. Cafmeyer, P. Guyon, M. O. Andreae, P. Artaxo and W. Maenhaut, *Science*, 2004, **303**, 1173–1176.

17 P. J. Ziemann and R. Atkinson, *Chem. Soc. Rev.*, 2012, **41**, 6582–6605.

18 V. Choudhary, T. Gupta and R. Zhao, *ACS Earth and Space Chemistry*, 2022, **6**, 2335–2347.

19 V. Choudhary, M. Loebel Roson, X. Guo, T. Gautam, T. Gupta and R. Zhao, *Environ. Sci.: Atmos.*, 2023, –.

20 B. Yuan, A. R. Koss, C. Warneke, M. Coggon, K. Sekimoto and J. A. de Gouw, *Chemical Reviews*, 2017, **117**, 13187–13229.

21 A. Bierbach, I. Barnes, K. H. Becker and E. Wiesen, *Environmental science & technology*, 1994, **28**, 715–729.

22 L. Wang, J. G. Slowik, N. Tripathi, D. Bhattu, P. Rai, V. Kumar, P. Vats, R. Satish, U. Baltensperger, D. Ganguly, N. Rastogi, L. K. Sahu, S. N. Tripathi and A. S. H. Prévôt, *Atmospheric Chemistry and Physics*, 2020, **20**, 9753–9770.

23 M. M. Coggon, C. Y. Lim, A. R. Koss, K. Sekimoto, B. Yuan, J. B. Gilman, D. H. Hagan, V. Selimovic, K. J. Zarzana, S. S. Brown, J. M. Roberts, M. Müller, R. Yokelson, A. Wisthaler, J. E. Krechmer, J. L. Jimenez, C. Cappa, J. H. Kroll, J. de Gouw and C. Warneke, *Atmospheric Chemistry and Physics*, 2019, **19**, 14875–14899.

24 Z. C. J. Decker, S. Wang, I. Bourgeois, P. Campuzano Jost, M. M. Coggon, J. P. DiGangi, G. S. Diskin, F. M. Flocke, A. Franchin, C. D. Fredrickson, G. I. Gkatzelis, S. R. Hall, H. Halliday, K. Hayden, C. D. Holmes, L. G. Huey, J. L. Jimenez, Y. R. Lee, J. Lindaas, A. M. Middlebrook, D. D. Montzka, J. A. Neuman, J. B. Nowak, D. Pagonis, B. B. Palm, J. Peischl, F. Piel, P. S. Rickly, M. A. Robinson, A. W. Rollins, T. B. Ryerson, K. Sekimoto, J. A. Thornton, G. S. Tyndall, K. Ullmann, P. R. Veres, C. Warneke, R. A. Washenfelder, A. J. Weinheimer, A. Wisthaler, C. Womack and S. S. Brown, *Environmental Science & Technology*, 2021, **55**, 15646–15657.

25 P. S. Rickly, M. M. Coggon, K. C. Aikin, R. J. I. Alvarez, S. Baidar, J. B. Gilman, G. I. Gkatzelis, C. Harkins, J. He, A. Lamplugh, A. O. Langford, B. C. McDonald, J. Peischl, M. A. Robinson, A. W. Rollins, R. H. Schwantes, C. J. Senff, C. Warneke and S. S. Brown, *Environmental Science & Technology*, 2023, **57**, 1257–1267.

26 E. A. Bruns, J. G. Slowik, I. El Haddad, D. Kilic, F. Klein, J. Dommen, B. Temime-Roussel, N. Marchand, U. Bal-

tensperger and A. S. H. Prévôt, *Atmospheric Chemistry and Physics*, 2017, **17**, 705–720.

27 A. C. D. Rivett and N. V. Sidgwick, *J. Chem. Soc., Trans.*, 1910, **97**, 1677–1686.

28 B. R. T. Simoneit, M. Kobayashi, M. Mochida, K. Kawamura, M. Lee, H.-J. Lim, B. J. Turpin and Y. Komazaki, *Journal of Geophysical Research: Atmospheres*, 2004, **109**,.

29 A. W. H. Chan, K. E. Kautzman, P. S. Chhabra, J. D. Surratt, M. N. Chan, J. D. Crounse, A. Kürten, P. O. Wennberg, R. C. Flagan and J. H. Seinfeld, *Atmospheric Chemistry and Physics*, 2009, **9**, 3049–3060.

30 K. E. Kautzman, J. D. Surratt, M. N. Chan, A. W. H. Chan, S. P. Hersey, P. S. Chhabra, N. F. Dalleska, P. O. Wennberg, R. C. Flagan and J. H. Seinfeld, *The Journal of Physical Chemistry A*, 2010, **114**, 913–934.

31 T. E. Kleindienst, M. Jaoui, M. Lewandowski, J. H. Offenberg and K. S. Docherty, *Atmospheric Chemistry and Physics*, 2012, **12**, 8711–8726.

32 M. Shrivastava, S. Lou, A. Zelenyuk, R. C. Easter, R. A. Corley, B. D. Thrall, P. J. Rasch, J. D. Fast, S. L. M. Simonich, H. Shen and S. Tao, *Proceedings of the National Academy of Sciences*, 2017, **114**, 1246–1251.

33 Q. Mu, M. Shiraiwa, M. Octaviani, N. Ma, A. Ding, H. Su, G. Lammel, U. Pöschl and Y. Cheng, *Science Advances*, 2018, **4**, eaap7314.

34 B. Simoneit, J. Schauer, C. Nolte, D. Oros, V. Elias, M. Fraser, W. Rogge and G. Cass, *Atmospheric Environment*, 1999, **33**, 173–182.

35 B. R. Simoneit, *Applied Geochemistry*, 2002, **17**, 129–162.

36 H. Bhattarai, E. Saikawa, X. Wan, H. Zhu, K. Ram, S. Gao, S. Kang, Q. Zhang, Y. Zhang, G. Wu, X. Wang, K. Kawamura, P. Fu and Z. Cong, *Atmospheric Research*, 2019, **220**, 20–33.

37 Y. Chen, P. McDaid and L. Deng, *Chemical Reviews*, 2003, **103**, 2965–2984.

38 H. O. T. Pye, A. Nenes, B. Alexander, A. P. Ault, M. C. Barth, S. L. Clegg, J. L. Collett Jr., K. M. Fahey, C. J. Hennigan, H. Herrmann, M. Kanakidou, J. T. Kelly, I.-T. Ku, V. F. McNeill, N. Riemer, T. Schaefer, G. Shi, A. Tilgner, J. T. Walker, T. Wang, R. Weber, J. Xing, R. A. Zaveri and A. Zuend, *Atmospheric Chemistry and Physics*, 2020, **20**, 4809–4888.

39 M. Shiraiwa, Y. Li, A. P. Tsimpidi, V. A. Karydis, T. Berkemeier, S. N. Pandis, J. Lelieveld, T. Koop and U. Pöschl, *Nature Communications*, 2017, **8**, 15002.

40 C. E. Kolb, R. A. Cox, J. P. D. Abbatt, M. Ammann, E. J. Davis, D. J. Donaldson, B. C. Garrett, C. George, P. T. Griffiths, D. R. Hanson, M. Kulmala, G. McFiggans, U. Pöschl, I. Riipinen, M. J. Rossi, Y. Rudich, P. E. Wagner, P. M. Winkler, D. R. Worsnop and C. D. O' Dowd, *Atmospheric Chemistry and Physics*, 2010, **10**, 10561–10605.

41 M. B. Fernandes, J. O. Skjemstad, B. B. Johnson, J. D. Wells and P. Brooks, *Chemosphere*, 2003, **51**, 785–795.

42 J. F. Pankow, *Atmospheric Environment*, 1994, **28**, 185–188.

43 V. H. Grassian, *International Reviews in Physical Chemistry*, 2001, **20**, 467–548.

44 U. Pöschl, Y. Rudich and M. Ammann, *Atmospheric Chemistry and Physics*, 2007, **7**, 5989–6023.

45 T. Moise and Y. Rudich, *Journal of Geophysical Research: Atmospheres*, 2000, **105**, 14667–14676.

46 J. Park, A. L. Gomez, M. L. Walser, A. Lin and S. A. Nizkorodov, *Phys. Chem. Chem. Phys.*, 2006, **8**, 2506–2512.

47 J. He, B. Zielinska and R. Balasubramanian, *Atmospheric Chemistry and Physics*, 2010, **10**, 11401–11413.

48 J. J. Schauer, M. P. Fraser, G. R. Cass and B. R. T. Simoneit, *Environmental Science & Technology*, 2002, **36**, 3806–3814.

49 P. M. Fine, B. Chakrabarti, M. Krudysz, J. J. Schauer and C. Sioutas, *Environmental Science & Technology*, 2004, **38**, 1296–1304.

50 Y.-L. Zhang, K. Kawamura, T. Watanabe, S. Hatakeyama, A. Takami and W. Wang, *Atmospheric Environment*, 2016, **140**, 147–149.

51 D. Hoffmann, Y. Iinuma and H. Herrmann, *Journal of Chromatography A*, 2007, **1143**, 168–175.

52 B. Rooney, R. Zhao, Y. Wang, K. H. Bates, A. Pillarisetti, S. Sharma, S. Kundu, T. C. Bond, N. L. Lam, B. Ozaltun, L. Xu, V. Goel, L. T. Fleming, R. Weltman, S. Meinardi, D. R. Blake, S. A. Nizkorodov, R. D. Edwards, A. Yadav, N. K. Arora, K. R. Smith and J. H. Seinfeld, *Atmospheric Chemistry and Physics*, 2019, **19**, 7719–7742.

53 A. P. Mouat, C. Paton-Walsh, J. B. Simmons, J. Ramirez-Gamboa, D. W. T. Griffith and J. Kaiser, *Atmospheric Chemistry and Physics*, 2022, **22**, 11033–11047.

54 J. Y. Lee, D. A. Lane, J. B. Heo, S.-M. Yi and Y. P. Kim, *Atmospheric Environment*, 2012, **55**, 17–25.

55 G. D. Smith, E. Woods, C. L. DeForest, T. Baer and R. E. Miller, *The Journal of Physical Chemistry A*, 2002, **106**, 8085–8095.

56 J. D. Hearn and G. D. Smith, *The Journal of Physical Chemistry A*, 2004, **108**, 10019–10029.

57 S. Gross, R. Iannone, S. Xiao and A. K. Bertram, *Phys. Chem. Chem. Phys.*, 2009, **11**, 7792–7803.

58 T. Nah, S. H. Kessler, K. E. Daumit, J. H. Kroll, S. R. Leone and K. R. Wilson, *The Journal of Physical Chemistry A*, 2014, **118**, 4106–4119.

59 T. Berkemeier, A. Mishra, C. Mattei, A. J. Huisman, U. K. Krieger and U. Pöschl, *ACS Earth and Space Chemistry*, 2021, **5**, 3313–3323.

60 J. N. Crowley, M. Ammann, R. A. Cox, R. G. Hynes, M. E. Jenkin, A. Mellouki, M. J. Rossi, J. Troe and T. J. Wallington, *Atmospheric Chemistry and Physics*, 2010, **10**, 9059–9223.

61 F. A. Houle, W. D. Hinsberg and K. R. Wilson, *Phys. Chem. Chem. Phys.*, 2015, **17**, 4412–4423.

62 D. A. Knopf, U. Pöschl and M. Shiraiwa, *Analytical Chemistry*, 2015, **87**, 3746–3754.

63 M. J. Tang, M. Shiraiwa, U. Pöschl, R. A. Cox and M. Kalberer, *Atmospheric Chemistry and Physics*, 2015, **15**, 5585–5598.

64 J. Li, S. M. Forrester and D. A. Knopf, *Atmospheric Chemistry and Physics*, 2020, **20**, 6055–6080.

65 S. Jennings, *Journal of Aerosol Science*, 1988, **19**, 159–166.

66 N. FUCHS and A. SUTUGIN, *Topics in Current Aerosol Re-*

search, Pergamon, 1971, p. 1.

67 R. Zhao, C. M. Kenseth, Y. Huang, N. F. Dalleska, X. M. Kuang, J. Chen, S. E. Paulson and J. H. Seinfeld, *The Journal of Physical Chemistry A*, 2018, **122**, 5190–5201.

68 R. Zhao, A. K. Y. Lee, C. Wang, F. Wania, J. P. S. Wong, S. Zhou and J. P. D. Abbatt, in *The Role of Water in Organic Aerosol Multiphase Chemistry: Focus on Partitioning and Reactivity*, 2017, ch. 2, pp. 95–184.

69 J. H. Hu, Q. Shi, P. Davidovits, D. R. Worsnop, M. S. Zahniser and C. E. Kolb, *The Journal of Physical Chemistry*, 1995, **99**, 8768–8776.

70 Q. Zou, H. Song, M. Tang and K. Lu, *Chinese Chemical Letters*, 2019, **30**, 2236–2240.

71 J. Liggio and S.-M. Li, *Journal of Geophysical Research: Atmospheres*, 2006, **111**,.

72 A. Jammoul, S. Gligorovski, C. George and B. D'Anna, *The Journal of Physical Chemistry A*, 2008, **112**, 1268–1276.

73 S. A. Styler, M. Brigante, B. D'Anna, C. George and D. J. Donaldson, *Phys. Chem. Chem. Phys.*, 2009, **11**, 7876–7884.

74 M. Abou-Ghanem, A. O. Oliynyk, Z. Chen, L. C. Matchett, D. T. McGrath, M. J. Katz, A. J. Locock and S. A. Styler, *Environmental Science & Technology*, 2020, **54**, 13509–13516.

75 A. M. Arangio, J. H. Slade, T. Berkemeier, U. Pöschl, D. A. Knopf and M. Shiraiwa, *The Journal of Physical Chemistry A*, 2015, **119**, 4533–4544.

76 G. Gržinić, T. Bartels-Rausch, T. Berkemeier, A. Türler and M. Ammann, *Atmospheric Chemistry and Physics*, 2015, **15**, 13615–13625.

77 L. A. Goldberger, L. G. Jahl, J. A. Thornton and R. C. Sullivan, *Environ. Sci.: Processes Impacts*, 2019, **21**, 1684–1698.

78 J. Rissler, A. Vestin, E. Swietlicki, G. Fisch, J. Zhou, P. Artaxo and M. O. Andreae, *Atmospheric Chemistry and Physics*, 2006, **6**, 471–491.

79 R. P. Staiger and E. B. Miller, *The Journal of Organic Chemistry*, 1959, **24**, 1214–1219.

80 P. Jain, D. Castellanos-Acuna, S. C. P. Coogan, J. T. Abatzoglou and M. D. Flannigan, *Nature Climate Change*, 2022, **12**, 63–70.